Chinese Chemical Letters 34 (2023) 107472

Contents lists available at ScienceDirect

Chinese Chemical Letters

journal homepage: www.elsevier.com/locate/cclet

Aniline as a TICT rotor to derive methine fluorogens for biomolecules: A curcuminoid-BF_2 compound for lighting up HSA/BSA

Yue Zhang[a,b], Wei Zhou[b], Ning Xu[b], Guangying Wang[b], Jin Li[b], Kai An[b], Wenchao Jiang[b], Xuelian Zhou[b], Qinglong Qiao[b,*], Xindong Jiang[a,*], Zhaochao Xu[b,*]

[a] Liaoning & Shenyang Key Laboratory of Functional Dye and Pigment, Shenyang University of Chemical Technology, Shenyang 110142, China
[b] CAS Key Laboratory of Separation Science for Analytical Chemistry, Dalian Institute of Chemical Physics, Chinese Academy of Sciences, Dalian 116023, China

ARTICLE INFO

Article history:
Received 18 April 2022
Revised 22 April 2022
Accepted 24 April 2022
Available online 28 April 2022

Keywords:
Fluorogen
Aniline
TICT
HSA
Methine dyes

ABSTRACT

The unique structure of fluorescent proteins in which the fluorophore is encapsulated by the protein shell to restrict rotation and emit light inspired the screening of chromophores that selectively bind to biomolecules to generate fluorescence. In this paper, we report a curcuminoid-BF_2-like fluorescent dye **N-BF_2** containing 4-dimethylaniline as an electron-donating group. When this dye is combined with HSA or BSA, the fluorescence is enhanced 90/112-fold, and the fluorescence quantum yield increases from <0.001 to 0.16/0.19. Such a large change in fluorescence enhancement is due to the encapsulation of **N-BF_2** in the protein cavity by HSA/BSA, which inhibits the intramolecular rotation of the aniline moiety caused by charge transfer after the fluorophore is excited by light. **N-BF_2** has fast and strong binding to HSA or BSA and was found to be reversible in solution and intracellularly. Since **N-BF_2** also has the ability to target lipid droplets, the complex of **N-BF_2**/HSA realizes the regulation of reversible lipid droplet staining in cells.

© 2022 Published by Elsevier B.V. on behalf of Chinese Chemical Society and Institute of Materia Medica, Chinese Academy of Medical Sciences.

The interaction between dyes and surrounding molecules and the process of photoexcitation lead to changes in the conjugated system or molecular configuration of dye molecules, resulting in fluorescence changes, which create the signal transduction mechanism of fluorescent probes [1–3]. With the coordinated development of labeling techniques and dye chemistry, fluorescent probes have been continuously updated, from general environment-sensitive fluorescence changes to selective fluorescence responses after molecular recognition for specific target molecules [4,5]. The most typical fluorophore with molecular recognition fluorescence response performance is the fluorescent protein [6]. The molecular recognition between its endogenous chromophore and the fluorescent protein cavity effectively inhibits the rotation of the chromophore in the protein cavity and produces a unique phenolic hydroxyl dehydrogenation reaction. The hydroxyl dehydrogenation reaction ensures that the chromophore can only have fluorescence emission ability in the GFP cavity [7]. Such chromophores that activate fluorescence through molecular recognition are called fluorogens. Drawing on the pattern of recognition and binding of such endogenous chromophores and biomolecules to emit light, in recent years, relying on the screening of substrate molecules by antibodies or aptamers, non-covalently bound fluorescent antibodies and aptamers activated against exogenous chromophores has been developed [8–11]. Depending on genetic coding and enzymatic reactions, covalently linked protein tags, such as the widely used SNAP-tag [11,12] and Halo-tag [13], have been developed. This strategy of combining and activating fluorogen emission has stimulated the study of fluorescent probes that recognize biological macromolecules (including proteins, nucleic acids and carbohydrates) with low background fluorescence, but how to realize molecular recognition and activate fluorescence is a challenge in the research of such fluorescent probes [14–18].

Inhibition of twisted intramolecular charge transfer (TICT) is one of the main mechanisms by which molecular recognition activates fluorescence, with dialiphatic substituted amino groups being the most commonly used rotors (Fig. 1a) [19–21]. The structure of such molecules is characterized by the direct conjugation of tertiary amine groups in planar rigid chromophores, common fluorophores such as coumarin, naphthalimide and rhodamine. The lone pair of electrons of the tertiary amine is delocalized to the aromatic system of the chromophore due to the effect of electron donating and acceptance, forming a partial C=N double bond. After being excited by light, an electron is completely intramolecularly transferred to the acceptor, and the tertiary amine group ro-

* Corresponding authors.
E-mail addresses: qqlqiao@dicp.ac.cn (Q. Qiao), xdjiang@syuct.edu.cn (X. Jiang), zcxu@dicp.ac.cn (Z. Xu).

https://doi.org/10.1016/j.cclet.2022.04.070
1001-8417/© 2022 Published by Elsevier B.V. on behalf of Chinese Chemical Society and Institute of Materia Medica, Chinese Academy of Medical Sciences.

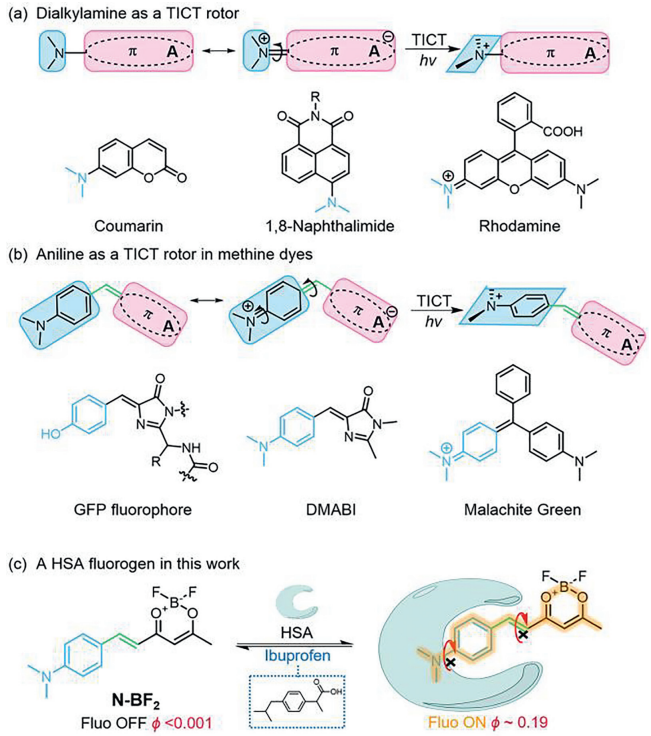

Fig. 1. (a) The fluorophores with dialkylamine as a TICT rotator. (b) Aniline as a TICT rotor in methine dyes. (c) HSA probe with aniline as a TICT rotator in this work.

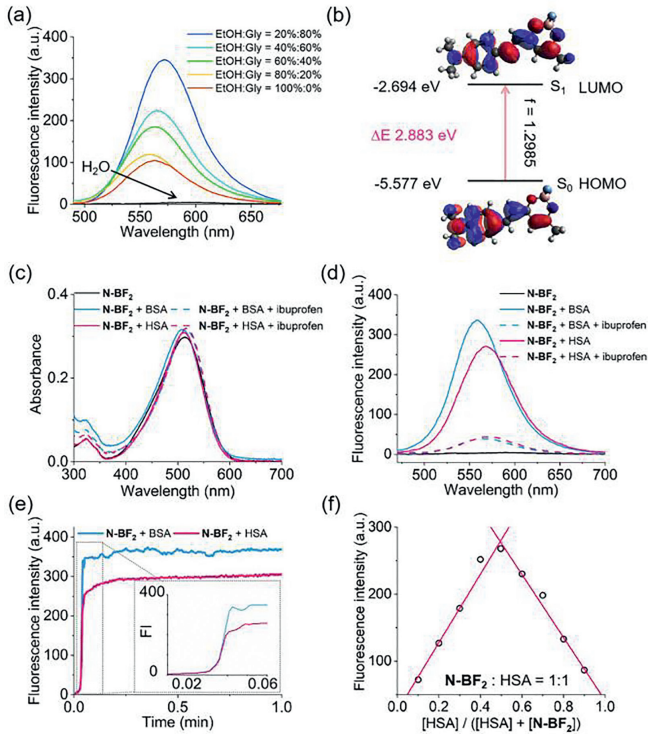

Fig. 2. (a) Fluorescence spectra of **N-BF$_2$** in different proportions of glycerol/EtOH mixture and H_2O. (b) Molecular orbital amplitude plots of HOMO and LUMO energy levels of **N-BF$_2$**. (c) The absorption and (d) fluorescence spectra of **N-BF$_2$** upon addition of HSA/BSA and pretreated with ibuprofen (200 μmol/L). (e) Time course of fluorescence intensity of 5 μmol/L **N-BF$_2$** in the presence of 5 μmol/L HSA and BSA. (f) The Job's plot of **N-BF$_2$** and HSA at diffffferent ratios, total concentration of **N-BF$_2$** and HSA was 10 μmol/L. λ_{ex} = 460 nm.

tates to form a vertical configuration with the chromophore to stabilize the zwitterion with intramolecular charge separation. However, such molecules typically have high background fluorescence and lack strong binding to biomolecules due to their large size and structural rigidity.

Reducing the size of the chromophore, and increasing the flexibility of the molecule is a conventional improvement idea (Fig. 1b). The fluorophore of the fluorescent protein is connected a methine group to a single benzene ring conjugated a system as the electron donor and acceptor, respectively. The existence of the methine group increases the flexibility when it is combined with biomolecules, and the size of the conjugated structure of the single benzene ring is moderate. This type of methionine chromophore has the structural characteristics of strong binding force with biological macromolecules. Inspired by fluorescent protein chromophores, aniline-substituted methine chromophores, with typical structures such as DMABI and Malachite Green, have been shown to have strong binding to both proteins and nucleic acids [22,23]. More importantly, aniline acts as an electron-donating group to form a quinoid structure, and the tertiary amine group and the aniline as a whole can co-rotate during the intramolecular charge transfer process in the excited state, which can more effectively quench the fluorescence. The background fluorescence of these chromophores is very low, and the fluorescence intensity increases by 2–3 orders of magnitude after binding to proteins or nucleic acids. In one of our recent works, the importance of the methine structure in binding to biomacromolecules and activating fluorescence was also demonstrated through the modification of the methine structure in the fluorophore by linking electron-donating and electron-withdrawing groups.

In this paper, we introduced aniline into the difluoroboron β-diketonate chromophore *via* a methine bridge, resulting in **N-BF$_2$** that is almost non-fluorescent in aqueous solution (Fig. 1c). **N-BF$_2$** has fast and strong binding to HSA or BSA, accompanied by the activation of fluorescence (fluorescence enhancement 90 (HSA)/112 (BSA)-fold). This intermolecular binding was found to be rapid and reversible in solution and intracellularly. Since **N-BF2** also has lipid droplet-targeted ability,the complex of **N-BF$_2$**/HSA realizes the regulation of reversible lipid droplets staining in cells.

Firstly, we inspected the quenching effect of aniline-rotor in **N-BF$_2$**, through the analysis of fluorescence spectra depending on different solvents and viscosity. Similar with the most traditional D-π-A dyes, **N-BF$_2$** shown solvochromic effect with obvious red-shift in fluorescence emission from 541 nm in dioxane to 591 nm in DMSO (Fig. S1 in Supporting information). And it should be noted that **N-BF$_2$** exhibited negligible fluorescence in strong polar solvent (ϕ < 0.01) which indicated the facile formation of TICT and its low background (Fig. 2a and Table S1 in Supporting information). This was further illustrated through the electron density changing in LUMO and HOMO (Fig. 2b). Once excited, the electron density of aniline decreased and flowed toward difluoroboron β-diketonate thus enhancing the charge separation which favored to form TICT. While with the increase of viscosity, the corresponding emission intensity of **N-BF$_2$** significantly enhanced (Fig. 2a). Such viscosity-dependent fluorescence intensification is also a typical characteristic of TICT emission. These results indicated potential applications of **N-BF$_2$** in developing fluorogenic probes based on restricted rotation.

Surprisingly, the rotation of aniline-rotor in **N-BF$_2$** can be inhibited upon binding HSA and BSA thus inducing great fluorescence enhancement. After the addition of HSA or BSA, the maximum absorption of **N-BF$_2$** at 513 nm slightly blue-shifted to 506 nm and 507 nm, respectively (Fig. 2c). Similarly, the emission at 583 nm blue-shifted to 568 nm and 559 nm, respectively, which indicated the polar microenvironment of cavity binding the chromophore

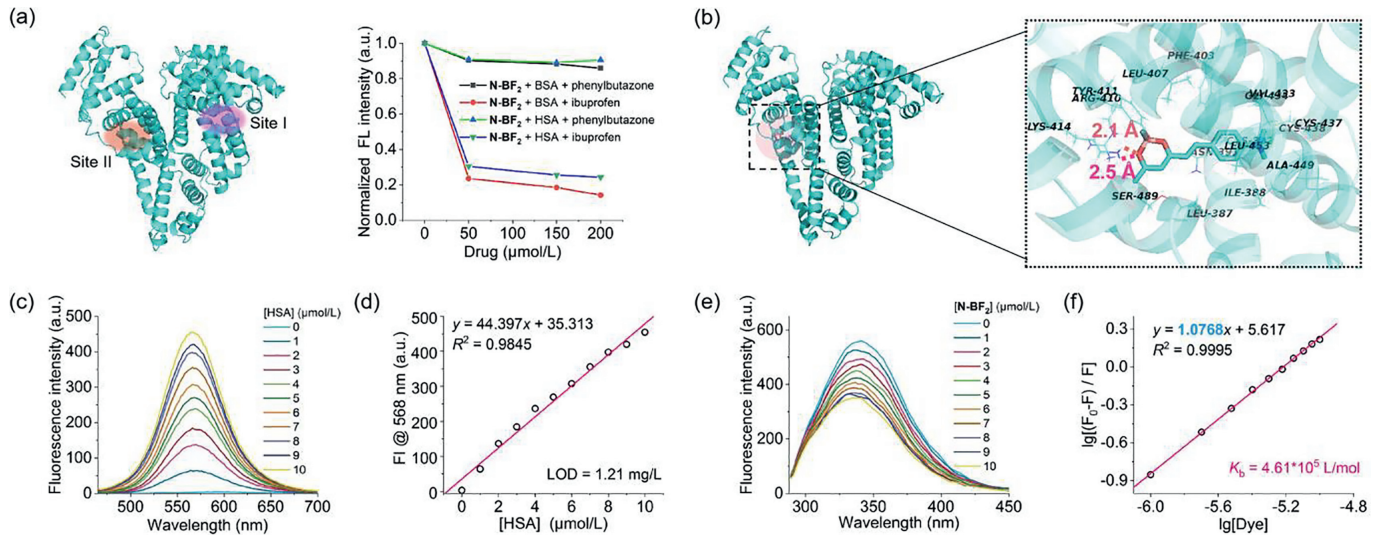

Fig. 3. (a) Normalized fluorescence intensity of **N-BF$_2$** (5 μmol/L) in presence of HSA (5 μmol/L) or BSA (5 μmol/L) which pretreated with different concentrations of site-specific marker (0–200 μmol/L ibuprofen or phenylbutazone). (b) Binding modes of **N-BF$_2$** with contacting residues in binding site II of HSA. (c) Fluorescence spectra of **N-BF$_2$** (5 μmol/L) in presence of different concentration of HSA (0–10 μmol/L). (d) The linear relationship of fluorescence intensity at 568 nm with concentration of HSA (0–10 μmol/L). λ_{ex} = 460 nm. (e) Fluorescence emission spectra of HSA (5 μmol/L) in presence of increasing concentration of **N-BF$_2$** (0–10 μmol/L) and (f) double logarithmic relationship of fluorescence intensity at 340 nm with the concentration of **N-BF$_2$** (0–10 μmol/L). λ_{ex} = 280 nm.

(Fig. 2d). In the meanwhile, the fluorescence intensity increased more than 90-fold (HSA) and 112-fold (BSA), respectively (Table S2 in Supporting information). We also found **N-BF$_2$** could sense HSA and BSA in ~1.2 s much faster than those reported HSA/BSA probes (Fig. 2e and Table S3 in Supporting information). Furthermore, the Job's plot was conducted through monitoring fluorescence intensity at 568/559 nm, and indicated the **N-BF$_2$**/HSA and **N-BF$_2$**/BSA complexes all had 1:1 stoichiometry (Fig. 2f and Fig. S2 in Supporting information).

To further understand the binding between HSA and **N-BF$_2$**, drug competition and molecular docking experiments were next performed. Phenylbutazone and ibuprofen, which have been known to bind HSA/BSA at site I and site II, respectively, are used to inspect the binding model. Both **N-BF$_2$**/HSA and **N-BF$_2$**/BSA complexes shown slight decrease in presence of 50–200 μmol/L phenylbutazone. However, the addition of ibuprofen could induce the fluorescence intensity of **N-BF$_2$** sharply decreased to 30% (Fig. 3a). It indicated that **N-BF$_2$** most likely to bind HSA/BSA at narrow site II which considered as the common drug sites. The following docking study between **N-BF$_2$** and HSA/BSA also demonstrated this result (Fig. 3b and Fig. S3 in Supporting information). It revealed that oxygen in difluoroboron β-diketonate could formed two stable hydrogen bonds of 2.1 Å and 2.5 Å with the basic amino acid Arg-410 and Lys-414, which made **N-BF$_2$** specifically bind site II. On the other side, hydrophobic interactions of aniline unit with surrounding neutral amino acids, Phe-403, Val-433, Leu-453, Ala-449, Cys-438, Cys-392 and Ile-388, were found thus inhibiting the rotation of aniline and enhancing fluorescence intensity of **N-BF$_2$**. Inspired by the stable binding model, titration experiment and double logarithmic equation was further conducted to examine the limit of detection (LOD) and binding constant (K_b). With the addition of HSA, the fluorescence intensity gradually enhanced and the emission wavelength shifted from 583 nm to 568 nm (Fig. 3c). A linear relationship (R^2 = 0.9845) was found between fluorescence intensity of **N-BF$_2$** and HSA concentration in the range of 0–10 μmol/L (Fig. 3d). Based on $3\sigma/k$, the corresponding limit of detection (LOD) for HSA was calculated to be 1.21 mg/mL (Fig. 3d). Besides, with the addition of **N-BF$_2$**, the fluorescence intensity at 340 nm gradually decreased and the concentration-dependent fluorescence changes were utilized to find the binding constant, the K_b was

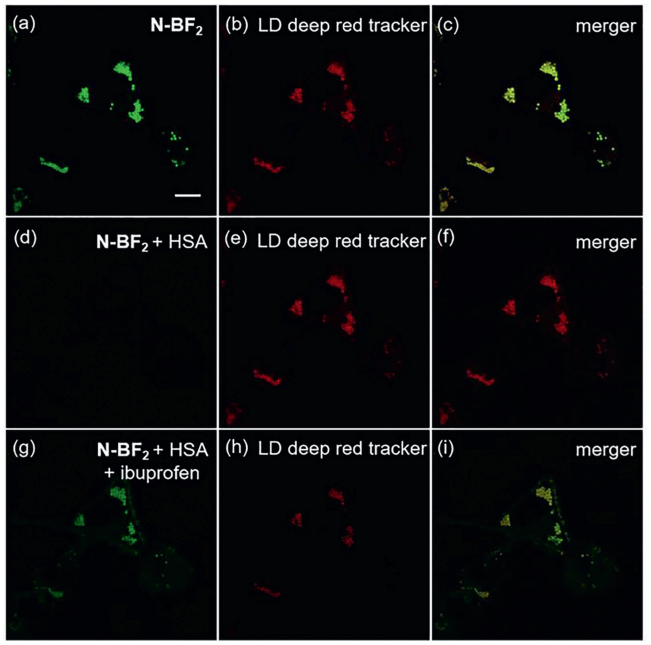

Fig. 4. Confocal cellular imaging of 1 μmol/L **N-BF$_2$** in HeLa cells in presence or absence of HSA and ibuprofen. [HSA] = 30 μmol/L. [Ibuprofen] = 30 μmol/L. Scale bar = 10 μm.

4.61 × 10^5 L/mol (Figs. 3e and f). LOD and K_b of **N-BF$_2$** toward BSA was also inspected to be 0.93 mg/mL and 4.67 × 10^5 L/mol which indicated the strong chelation between HSA/BSAand **N-BF$_2$** (Figs. S4 and S5 in Supporting information). As an endogenous substance *in vivo*, HSA not only has high stability but also acts as a drug carrier which can increase the water solubility of drugs and regulate drug release. Therefore, we used **N-BF$_2$**/HSA complexes as a trigger to control the entry and exit of **N-BF$_2$** in living cells. As shown in Figs. 4a–c, **N-BF$_2$** could specifically light up lipid droplets in HeLa cells. With the addition of 30 μmol/L HSA, the fluorescence of **N-BF$_2$** in lipid droplets disappeared, indicating that **N-BF$_2$** gradually dissociated from lipid droplets and flowed out of cells to bind HSA (Figs. 4d–f). Ibuprofen could bind HSA with higher affinity. Then

the addition of ibuprofen replaced **N-BF$_2$** from HSA and the released **N-BF$_2$** could re-cross the cell membrane and go back into lipid droplets which had been confirmed by the recovery of fluorescence in lipid droplets (Figs. 4g–i). So, it could be concluded that the complex of **N-BF$_2$**/HSA indeed realized the regulation of reversible lipid droplet staining in cells.

In conclusion, we developed a fluorogenic HSA/BSA probe through introducing aniline and a methine bridge into the difluoroboron β-diketonate chromophore. Due to the inhibition of aniline rotation, **N-BF$_2$** could light up HSA/BSA in 1.2 s with 90/112-fold fluorescence enhancements. Furthermore, the stable hydrogen bonds made **N-BF$_2$** exhibit high sensitivity with HSA and K_b towards site II of HSA/BSA, with LOD 1.21/0.93 mg/mL, K_b $4.61 \times 10^5/4.67 \times 10^5$ L/mol, which had been confirmed by molecular docking experiments. Finally, we realized the regulation of reversible lipid droplets staining through binding and dissociation between **N-BF$_2$** and HSA in living cells, which may be applied in drug site-specific delivery.

Declaration of competing interest

The authors declare that they have no known competing financial interests or personal relationships that could have appeared to influence the work reported in this paper.

Acknowledgment

This work is supported by the National Natural Science Foundation of China (Nos. 22078314, 21878286, 21908216, 22078201, U1908202).

Supplementary materials

Supplementary material associated with this article can be found, in the online version, at doi:10.1016/j.cclet.2022.04.070.

References

[1] H. Singh, K. Tiwari, R. Tiwari, et al., Chem. Rev. 119 (2019) 11718–11760.
[2] Z. Xu, J. Yoon, D.R. Spring, Chem. Soc. Rev. 39 (2010) 1996–2006.
[3] W. Zhou, X. Fang, Q. Qiao, et al., Chin. Chem. Lett. 32 (2021) 943–946.
[4] J. Chen, W. Liu, X. Fang, et al., Chin. Chem. Lett. 33 (2022) 5042–5046.
[5] J. Chen, C. Wang, W. Liu, et al., Angew. Chem. Int. Ed. 60 (2021) 25104–25113.
[6] R.Y. Tsien, Angew. Chem. Int. Ed. 48 (2009) 5612–5626.
[7] D.P. Barondeau, C.D. Putnam, C.J. Kassmann, et al., Proc. Natl. Acad. Sci. U. S. A. 100 (2003) 12111–12116.
[8] C. Szent-Gyorgyi, B.F. Schmidt, Y. Creeger, et al., Nat. Biotechnol. 26 (2008) 235–240.
[9] E. Gallo, Bioconjug. Chem. 31 (2020) 16–27.
[10] L. Jullien, A. Gautier, Methods Appl. Fluoresc. 3 (2015) 042007.
[11] S. Xu, H.Y. Hu, Acta Pharmacol. Sin. 8 (2018) 339–348.
[12] W. Liu, Q. Qiao, J. Zheng, et al., Biosens. Bioelectron. 176 (2021) 112886.
[13] C.G. England, H. Luo, W. Cai, Bioconjug. Chem. 26 (2015) 975–986.
[14] W. Liu, R. Li, F. Deng, et al., ACS Appl. Bio Mater. 4 (2021) 2104–2112.
[15] W. Chi, Q. Qiao, C. Wang, et al., Angew. Chem. Int. Ed. 59 (2020) 20215–20223.
[16] F. Deng, Q. Qiao, J. Li, et al., J. Phys. Chem. B 124 (2020) 7467–7474.
[17] F. Deng, L. Liu, W. Huang, et al., Spectrochim. Acta A Mol. Biomol. Spectrosc. 240 (2020) 118466–118474.
[18] Q. Qiao, W. Liu, J. Chen, et al., Angew. Chem. Int. Ed. 61 (2022) e202202961.
[19] C. Wang, W. Chi, Q. Qiao, et al., Chem. Soc. Rev. 50 (2021) 12656–12678.
[20] W. Liu, J. Chen, Q. Qiao, et al., Chin. Chem. Lett. 33 (2022) 4943–4947.
[21] X. Li, J. Zheng, W. Liu, et al., Chin. Chem. Lett. 31 (2020) 2937–2940.
[22] K. Ferreira, H.Y. Hu, V. Fetz, et al., Angew. Chem. Int. Ed. 56 (2017) 8272–8276.
[23] X. Tan, T.P. Constantin, K.L. Sloane, et al., J. Am. Chem. Soc. 139 (2017) 9001–9009.